

## Electronic Supplementary Information

# Interplay of Molecule–Substrate and Intermolecular Interactions in [5]Thiaheterohelicene Assembly on Ag(111)

Changqing Ye,<sup>a</sup> Takuma Hattori,<sup>a</sup> Yuji Hamamoto,<sup>ab</sup> Pawel Krukowski,<sup>c</sup> Akira Saito,<sup>a</sup> Hideji Osuga,<sup>d</sup> Yoshitada Morikawa,<sup>a</sup> and Yuji Kuwahara<sup>a</sup>

<sup>a</sup> Department of Precision Engineering, Graduate School of Engineering, The University of Osaka, 2-1 Yamada-oka, Suita 565-0871, Osaka, Japan.

<sup>b</sup> Department of Communication Engineering, Okayama Prefectural University, 111 Kuboki, Soja 719-1197, Okayama, Japan.

<sup>c</sup> Department of Solid State Physics, Faculty of Physics and Applied Informatics, University of Lodz, Pomorska 149/152, 90-236 Lodz, Poland.

<sup>d</sup> Faculty of Systems Engineering, Wakayama University, 930 Sakaedani, Wakayama 640-8510, Wakayama, Japan.

## Results of Molecular dynamics simulations

### Computational details

Molecular dynamics (MD) simulations were carried out using the LAMMPS package<sup>1</sup>. The general AMBER force field<sup>2,3</sup> (GAFF) was employed to describe interactions among atoms. The simulation cell dimensions were  $34.4 \times 34.0 \times 40.0 \text{ \AA}^3$ , and periodic boundary conditions were applied in all three directions. A flat Ag(111) surface was modeled by a graphene sheet with a lattice constant of  $2.46 \text{ \AA}$ . During the simulation, the graphene substrate was kept fixed, while the molecules were fully relaxed. The SHAKE algorithm<sup>4</sup> was employed to constrain all C–H bonds.

To investigate self-assembly behaviour of [5]TH, the temperature was controlled using the Nosé–Hoover thermostat<sup>5,6</sup> with a time step of 1 fs. The molecules were initially randomly distributed on the graphene substrate. An initial energy minimization was performed to eliminate unphysical atomic overlaps. The system was then equilibrated at 250 K for 2 ns and subsequently cooled to 80 K at a constant cooling rate of 100 K/ns. An additional equilibration was performed at 80 K for 0.5 ns, during which thermodynamic data were collected every 0.1 ps for further analysis.

Two-dimensional intermolecular interaction energy maps were constructed using dimer configurations extracted from simulations of two-molecule systems initialized from random configurations. The relative orientation of the two molecules was fixed: one molecule (*M*-[5]TH) was placed at the origin, while the second molecule was laterally displaced on a grid with a spacing of  $0.1 \text{ \AA}$ . No further structural relaxation was allowed, and the interaction energies were calculated using fixed molecular geometries.

## Results

To investigate the self-assembly behavior of *rac*-[5]TH, we first performed 100 independent MD simulations, each starting from different initial configurations involving either two different enantiomers (*M-M*) or two identical enantiomers (*M-P*). During equilibration at 250 K, two enantiomers diffuse across the surface and may approach to form dimers. In most cases, dimer formation occurred and the resulting dimers remained stable throughout the simulation. However, in a fraction of trajectories, transient dimer formation was observed: the molecules initially assembled into dimers but subsequently separated and remained as isolated monomers on the surface. This behavior contrasts with that of [7]TH, for which dimer formation is highly stable and nearly irreversible. For both homochiral (*M-M*) and heterochiral (*M-P*) systems, among 100 simulation samples, approximately 70% of the simulations resulted in stable dimer formation, while the remaining ~30% ended with monomers dispersed on the surface.

After cooling the systems to 80 K to match the STM measurement conditions, several distinct dimer configurations were identified (Fig. S1). In the homochiral system, five distinct dimer configurations were obtained from the simulations. Similarly, four distinct dimer configurations were identified in the heterochiral system. Mirror-image counterparts of all four configurations were observed, reflecting the chiral symmetry of heterochiral dimer formation. Among the identified dimer configurations, one homochiral and one heterochiral dimers exhibit geometric features consistent with the dimer motifs observed in STM images: **homo1**, in which the two molecules are rotated by approximately 180° with respect to each other, such that their concave edges face each other symmetrically, and **hetero2**, in which the molecules are rotated by about 90°, with the concave edge of one molecule facing the lateral side of the other. These configurations were therefore chosen as representative motifs for subsequent analysis of intermolecular interactions. Despite the diversity of observed dimer geometries, their intermolecular interaction energies ( $E_{\text{int}}$ ) are found to be closely spaced, about 10 meV, indicating weak energetic discrimination among different binding motifs.

In homochiral system, although **homo1** exhibits the strongest intermolecular interaction, as indicated by the lowest binding energy, it appears only rarely in the simulations, with a formation probability of approximately 4%. In contrast, **homo2**, in which dimers formed by the same enantiomers oriented in the same direction, which have slightly higher binding energies, dominate dimer formation with a probability of 61%. This discrepancy likely arises from a higher energy barrier that must overcome to achieve the face-to-face arrangement in **homo1**. By comparison, configurations such as **homo2** are more kinetically accessible and therefore occur more frequently. In the heterochiral system, **hetero1** is both the most frequently formed configuration in the MD simulations and the most stable in terms of intermolecular interaction energy. However, this motif is not observed in STM experiments. Instead, **hetero2**, which is slightly less stable energetically, closely resembles the experimentally observed packing motif. This discrepancy indicates that the dominant heterochiral dimer formed under intrinsic intermolecular interactions is not necessarily compatible with adsorption on Ag(111). Although **hetero1** is favourable in the absence of substrate constraints, its geometry likely requires deviations from the preferred adsorption sites and orientations imposed by the Ag(111) surface, rendering it unfavourable in the adsorbed state. In contrast, **hetero2** can be accommodated more

readily within the adsorption-site registry and uniform azimuthal orientation observed in STM, allowing it to act as the effective building block for surface-supported ordered structures.

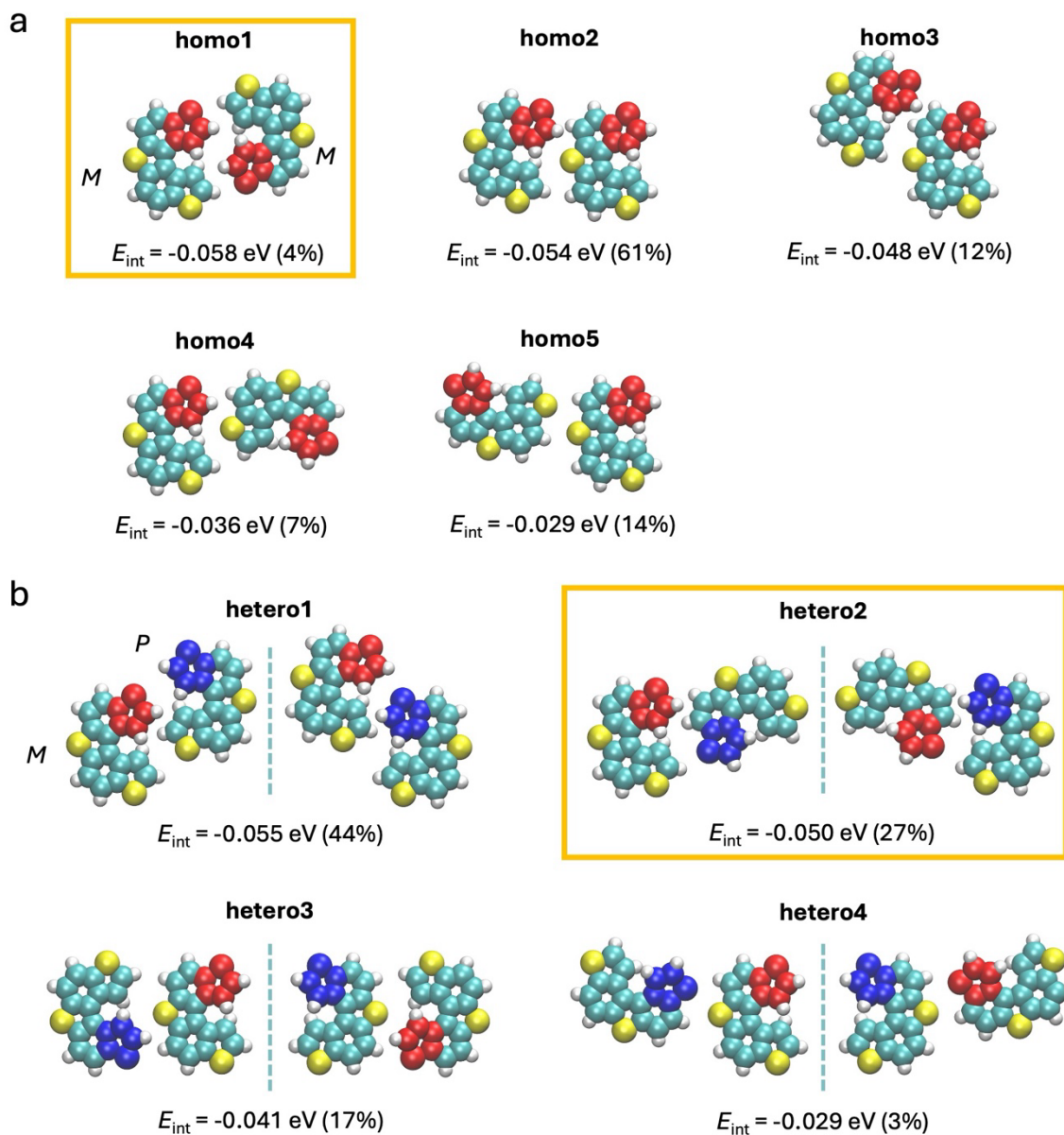


Fig. S1 Representative (a) homochiral and (b) heterochiral dimer configurations obtained from MD simulations, with the corresponding interaction energies and formation probabilities indicated below. To distinguish enantiomers, the molecule with a red hat is *M*-[5]TH, while that with a blue hat is *P*-[5]TH. In the heterochiral case, all configurations have mirror-image counterparts. The dimers highlighted by yellow frames correspond to those observed in STM images.

To further characterize the intermolecular interaction landscape, two-dimensional interaction energy maps were constructed for the representative homochiral and heterochiral

dimers, as shown in Fig. S2. One molecule (*M*-[5]TH) was fixed at the middle of the graphene substrate, while the second molecule was laterally displaced across the surface in the *xy*-plane on a grid with a step size of 0.1 Å. This approach is comparable to that used in the DFT calculations to explore intermolecular interactions in dimer systems. For both homochiral and heterochiral cases, two shallow energy minima were identified. The corresponding dimer configurations are consistent with those obtained from DFT calculations.

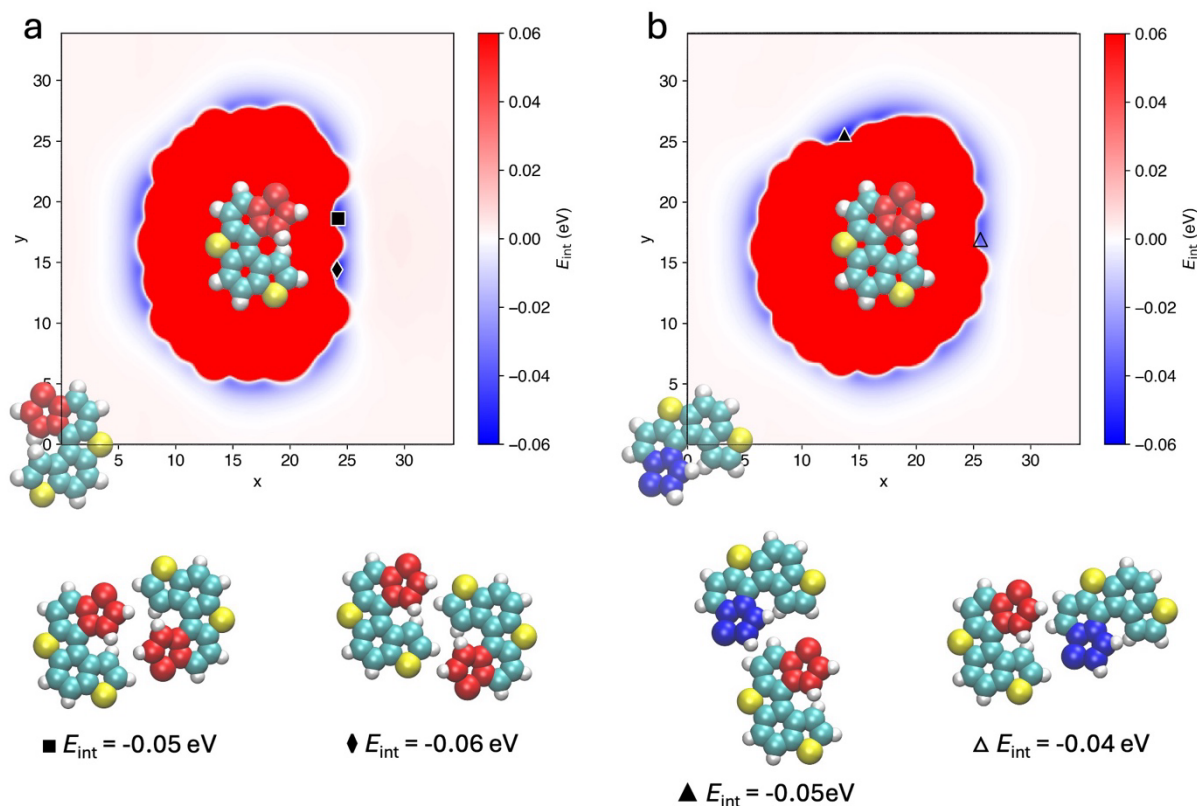


Fig. S2 Two-dimensional intermolecular interaction energy maps of (a) homochiral and (b) heterochiral dimers. Red regions in the maps indicate energetically forbidden areas where overlap occurs between molecules. The optimized dimer configurations corresponding to the energy minima are shown below the maps.

The number of molecules in the system was then increased to 4, 6, and 8 while keeping the unit cell fixed, corresponding to molecular densities of 0.34, 0.51, and 0.68 molecules/nm<sup>2</sup>, respectively. At eight molecules, the density matches that experimentally observed for the ordered structures (0.7 molecules/nm<sup>2</sup> for structure I, 0.69 molecules/nm<sup>2</sup> for structure II). However, even in the eight-molecule system, the molecules continuously rearranged on the surface, and no persistent long-range order emerged during the simulations (Fig. S3).

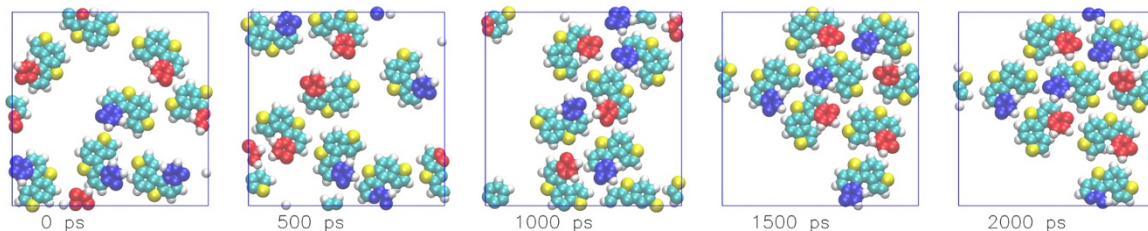


Fig. S3 Trajectory snapshots of eight [5]TH enantiomers. The graphene substrate is set to be transparent. During equilibration at 250 K, the molecules kept reorienting and rearranging into different configurations.

Taken together, these MD results indicate that while [5]TH molecules can form locally stable dimers with multiple nearly degenerate configurations, intermolecular interactions alone are insufficient to drive the formation of extended ordered structures. This contrasts with the behavior of [7]TH and highlights the essential role of molecule–substrate interactions in stabilizing the long-range ordered phases observed experimentally for [5]TH on Ag(111).

#### Reference

- 1 A. P. Thompson, H. M. Aktulga, R. Berger, D. S. Bolintineanu, W. M. Brown, P. S. Crozier, P. J. in 't Veld, A. Kohlmeyer, S. G. Moore, T. D. Nguyen, R. Shan, M. J. Stevens, J. Tranchida, C. Trott and S. J. Plimpton, *Computer Physics Communications*, 2022, **271**, 108171.
- 2 J. Wang, R. M. Wolf, J. W. Caldwell, P. A. Kollman and D. A. Case, *Journal of Computational Chemistry*, 2004, **25**, 1157–1174.
- 3 W. D. Cornell, P. Cieplak, Christopher, I. Bayly, I. R. Gould, K. M. Merz, D. M. Ferguson, D. C. Spellmeyer, T. Fox, J. W. Caldwell and P. A. Kollman, *Journal of the American Chemical Society*, 1995, **117**, 5179–5197.
- 4 H. C. Andersen, *Journal of Computational Physics*, 1983, **52**, 24–34.
- 5 W. G. Hoover, *Physical Review A*, 1985, **31**, 1695.
- 6 S. Nosé, *The Journal of Chemical Physics*, 1984, **81**, 511–519.